

****FULL TITLE****

*ASP Conference Series, Vol. **VOLUME**, **YEAR OF PUBLICATION***

****NAMES OF EDITORS****

Time-Evolving Photoionization: the Thin and Compact X-Ray Wind of NGC 4051

Fabrizio Nicastro¹, Martin Elvis, Nancy Brickhouse

Harvard-Smithsonian CfA, Cambridge, Massachusetts, USA;

¹*OAR-INAf, Monte Porzio Catone (RM), Italy*

Yair Krongold, Luc Binette

Instituto de Astronomia - UNAM, Mexico D.F., Mexico

Smita Mathur

Astronomy Department of Ohio State University, Columbus, Ohio, USA

Abstract. We discuss the power of time-evolving photoionization as a diagnostic tool to measure the electron density of photoionized gas. We apply this technique to a XMM-Newton observation of the ionized absorber in the Seyfert 1 galaxy NGC 4051, and present the first measurements of the its volume density, its distance from the central ionizing source, and so its mass outflow rate. By extrapolating these measurements to high-luminosity, large black hole mass, quasars, we speculate that AGN winds can play important roles both in the AGN-host-galaxy and AGN-IGM feedback processes.

1. Ionized AGN Winds: Open Questions

Ionized X-ray absorbers (*Warm Absorbers*: WAs) have been observed in the spectra of $\gtrsim 50$ % of Seyfert 1s (e.g. Crenshaw, Kraemer & George 2003) and quasars (Piconcelli et al. 2005). Such high detection rates, combined with evidence for transverse flows (Mathur et al. 1995; Crenshaw, Kraemer & George 2003) suggest that WAs are actually ubiquitous in AGN, but become directly visible in absorption only when our line of sight crosses the outflowing material. Despite their ubiquity, very little is still known about their physical state, dynamical strength and geometry. The most fundamental question is where do quasar winds originate? Addressing this question requires the independent determination of a quantity which is not directly observable: the electron density n_e of the outflowing material.

2. Time Evolving Photoionization

Recent studies have mostly shown that WAs are made up of just a few distinct physical components (e.g. Krongold et al., 2007 - K07 - and references therein). However, for each of these components, only average estimates of the product ($n_e R^2$) could be derived, from time-averaged spectral analyses. This is due

to the intrinsic degeneracy of n_e and R in the equation that defines the two observables: the ionization parameter of the gas $U_x = Q_x/(4\pi R^2 c n_e)$ and the luminosity of ionizing photons Q_x .

An unambiguous method to remove this degeneracy is to monitor the response of the ionization state of the gas in the wind to changes of the ionizing continuum (Krolik & Kriss 1995; Nicastro et al. 1999: hereinafter N99). Time-evolving photoionization equations define the Photoionization Equilibrium Time scale, t_{eq} , that measures the time necessary for the gas to reach photoionization equilibrium with the ionizing continuum (N99). This time-scale depends explicitly on the electron density n_e in the cloud, during both increasing and decreasing ionizing continuum phases (N99). Non-equilibrium photoionization models can therefore be used to measure the density of the gas n_e and, hence, its distance from the ionizing source.

Here, we apply this technique to a high S/N XMM-*Newton* observation of the low luminosity ($L_{bol} = 2.5 \times 10^{43}$ ergs s⁻¹, Ogle et al. 2004), low black hole mass ($M_{BH} = 1.9 \times 10^6 M_\odot$, Peterson et al. 2004), and rapidly (~ 1 hour) and highly (factor of ~ 10 , McHardy et al. 2004) X-ray variable Narrow Line Seyfert 1 NGC 4051.

3. The Variable Ionized Absorber of NGC 4051

NGC 4051 was observed for ~ 117 ks with the XMM-Newton Observatory, on 2001 May 16-17. The source varied by a factor of a few on timescales as short as 1 ks, and by a factor of ~ 12 from minimum to maximum flux over the whole observation (Fig. 1a). Details of the data reduction and analysis can be found in K07.

Two physically distinct but dynamically coincident ($v_{out} = 500$ km s⁻¹) WA phases were found in the average RGS spectrum of NGC 4051: a high- and a low-ionization phase (HIP and LIP).

3.1. Following the Time Variability of HIP and LIP

To study the response of the WAs of NGC 4051 to ionizing flux changes, we performed a time-resolved spectral analysis of 21 EPIC-PN spectra extracted from 21 distinct continuum levels ($a - u$, see Fig. 1b)¹. For both absorbing components the derived U_X values follow closely the source continuum lightcurve [compare panel (c) and (d) with panel (b) of Fig. 1], clearly indicating that the gas is responding quickly to the changes in the ionizing continuum.

To study more quantitatively how these changes are related to the changes in the continuum, we show in Fig. 2a,b the log of the source count rate ($\log C(t)$) vs. $\log U_X(t)$, for the HIP [panel (a)] and the LIP [panel (b)]. For most of the points of the HIP and for all the points of the LIP (within 2σ), $\log C(t)$ correlates with $\log U_X(t)$ tightly, which allows us to derive robust estimates of the quantity ($n_e R^2$) for both components (best fit lines in Fig. 2a,b, Table 1).

¹We checked, on average Low- and High-State (LS and HS in Fig. 1a) RGS and EPIC-PN spectra, that both detectors allowed the detection of WA opacity variations, and gave consistent results (see K07)

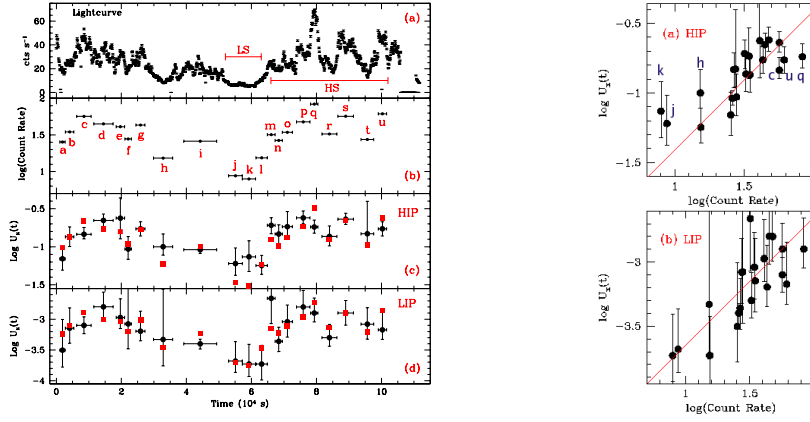


Figure 1. (left) Lightcurve of NGC 4051 in bins of 100 s [panel (a)]; Log of the count rate vs. time, for the 21 “flux states” used in this analysis [panel (b)]; Log of the ionization parameter of HIP [panel (c)] and LIP [panel (d)] as a function of time: filled squares are the expected value of U_X at equilibrium. Figure 2. (right) $\text{Log} U_X(t)$ vs. \log of the source count rate for the HIP [panel (a)] and the LIP [panel (b)].

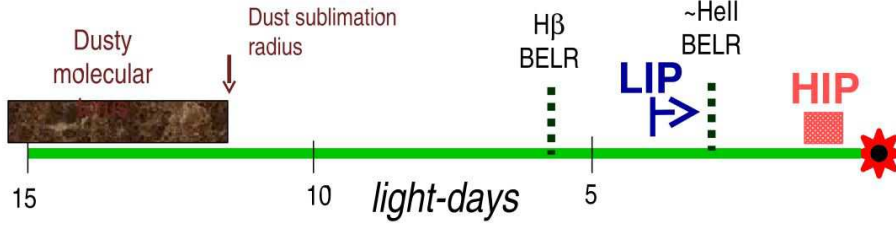


Figure 3. Location of features in the nuclear environment of NGC 4051 on a light-day scale.

Fig. 2a,b shows that the LIP is always in photoionization equilibrium with the ionizing flux, while the HIP deviates from photoionization equilibrium during periods of extreme flux states. Unlike the LIP, then (for which only an upper limit on t_{eq} , and so a lower limit on n_e , can be estimated), the behavior of the HIP allows us to set both lower and upper limits on $t_{eq}(HIP)$, and so on $n_e(HIP)$.

4. Results

From these independent estimates of n_e and $(n_e R^2)$, we can derive limits on R and so evaluate all physical and dynamical parameters of the gas, including the mass outflow rate. Table 1 summarizes our findings. Fig. 3 shows a schematic view of the location of the ionized outflow in NGC 4051. We find that:

Table 1. Physical and dynamical parameters of HIP and LIP of NGC 4051

Abs.	$(n_e R^2)$ 10^{38} cm^{-1}	n_e 10^7 cm^{-3}	P_e $10^{12} \text{ K cm}^{-3}$	R 10^{15} cm	ΔR 10^{14} cm	$(\Delta R/R)$	$\dot{M}_{out}/\dot{M}_{in}$ %
HIP	(0.38 ± 0.05)	$(0.58-2.1)$	$(2.9-10.5)$	$(1.3-2.6)$	$(1.9-7.2)$	$(0.1-0.2)$	$(2-3)$
LIP	(66 ± 3)	> 8.1	> 2.4	< 8.9	< 0.09	$< 10^{-3}$	< 2

- (1) time-evolving photoionization models are key diagnostics to measure the electron density in gas photoionized by variable X-ray sources;
- (2) the two X-ray WAs of NGC 4051 are both close to photoionization equilibrium, dense, compact and possibly in pressure balance (Fig. 3, Table 1);
- (3) the Narrow Emission Line Region (NELR), molecular torus and any radial continuous flow, are all ruled out as origin of the WAs of NGC 4051 (Fig. 3);
- (4) a static spherical configuration for the WAs of NGC 4051 is ruled out, and a dynamical but stationary spherical configuration (i.e. expulsion of thin spherical shells at regular time intervals) is highly unlikely, since it requires extremely fine tuning not to degenerate in a radial continuous flow;
- (5) the next simplest geometrical configuration, for the WAs of NGC 4051, is that of geometrically thin cone sections, originating in the accretion disk at a distance consistent with that of the high-ionization BLRs (Fig. 3; Elvis, 2000);
- (6) if this configuration applies to all AGN, then the presence or absence of WAs in the X-ray spectra of type 1 AGNs is explained simply by orientation, with WAs being visible only in those objects seen between edge-on and an angle equal to the disk-outflow angle;
- (7) the by-conical configuration is consistent with all our findings and provides reasonable values for the mass outflow rates of the WA of NGC 4051, relative to the source accretion rate: $\dot{M}_{out} = 2 - 5\% \dot{M}_{in}$ (Table 1);
- (8) these values, if extrapolated to high luminosity QSOs, suggest that WAs may play an important role in locally feeding the IGM with enriched material.

Finally, we note that a radial extension of disk winds toward larger disk radii, could produce cold absorption, as seen in type 2 AGNs (Risaliti, Elvis & Nicastro, 2002): in such objects WAs would be masked by the cold absorption, but the ionized wind would still shine in X-rays and could produce the photoionized X-ray cones observed in several Seyfert 2s (Guainazzi, this conference).

Acknowledgments. F.N. acknowledges support by NASA grant NNG05GK47G.

References

- Crenshaw, D. M., Kraemer, S. B., & George, I. M. 2003, A&A Rev., 41, 117
 Elvis, M. 2000, ApJ, 545, 63
 Krolik, J. H. & Kriss, G. A. 2001, ApJ, 561, 684
 Krongold, Y. et al. 2007, ApJ, in press
 Mathur, S., Elvis, M., & Wilkes, B. 1995, ApJ, 452, 230
 McHardy, I. M., et al. 2004, MNRAS, 348, 783
 Nicastro, F., Fiore, F., & Matt, G. 1999, ApJ, 517, 108
 Ogle, P. M. et al. 2004, ApJ, 606, 151
 Peterson B.M. et al. 2004, ApJ 613, 682
 Piconcelli, E. et al. 2005, A&A, 432, 15
 Risaliti, G., Elvis, M. & Nicastro, F., 2002, ApJ, 571, 234